Dennis Coughlin, Paul Jaffray, Mohammad Mansouri,
and Ajay Singh

Introduction

Facial trauma is a common presentation to the emergency department, usually as a result of blunt trauma. The trauma can range from a simple, isolated nondisplaced fracture to complex displaced facial fractures. Multiple fracture patterns have been described that make it easier to efficiently detect, document, and communicate the diagnosis in patients with multiple fractures. Rene Le Fort made the earliest and most famous classification in 1901, and since that time multiple other fracture patterns have been described [1]. While these can be present in pure form, often they coexist, particularly in the setting of high-impact trauma.

Paralleling this development in facial trauma classification has been that of surgical fixation. After the advent of antibiotics, the most commonly used treatment of complex facial fractures is open reduction. A primary reason for improvement in surgical treatment of facial fractures is the introduction and refinement of the concept of functional units of the face. This concept was first described

D. Coughlin, MD
Department of Radiology, UMass Memorial Health Care, Worcester, MA, USA

P. Jaffray
GBMC Healthcare, Baltimore, MD, USA

M. Mansouri, MD, MPH
Department of Radiology, Massachusetts General Hospital, 55 Fruit Street, Boston, MA 02114, USA

A. Singh, MD (✉)
Division of Emergency Radiology, Department of Radiology, Massachusetts General Hospital, 55 Fruit Street, Boston, MA 02114, USA

Harvard Medical School, Massachusetts General Hospital, 55 Fruit Street, Boston, MA 02114, USA
e-mail: asingh1@partners.org

by Sicher and DuBrul in 1970 [2]. Through experience surgeons have learned that reducing these functional units leads to the best anatomical and functional outcome for facial fractures [3–5].

While physical exam is an essential component in the workup of a trauma patient, this is often difficult due to the patient's mental state, distracting injuries, and associated comorbidities. Imaging plays a central role in the workup of the trauma patient. This is particularly true with the advent of modern multidetector CT scans.

Imaging of Craniofacial Trauma

Historically, initial assessment of facial trauma was performed with a facial radiograph series. Typical series included Caldwell, straight PA, Waters, Towne, lateral, and SMV views [6]. Radiographs are still being utilized, but their use has progressively diminished as CT technology continues to improve. In many institutions, the use of CT has largely replaced radiographs in the evaluation of the trauma patient. MRI is rarely used in the immediate workup of the trauma patient but can aid in evaluating complications.

Older generation CT scanners acquired axial images with subsequent patient repositioning required to obtain series in other planes. With improvement of imaging technology, helical acquisition on modern multi-slice CT scanners rapidly obtains a volume of data from which can be used to obtain reformations in any plane. Multiplanar imaging greatly aids in the detection and appropriate description of facial injuries.

Our CT trauma protocol for imaging of the head and maxillofacial region involves acquiring a data volume at 0.6 mm slice thickness from immediately below the mental protuberance to the skull vertex without intravenous contrast. Maxillofacial thin overlapping axial reconstructions as well as coronal and sagittal reformats, typically 2×1.5 mm, are generated using both bone and soft tissue algorithms. In addition, volume-rendered 3D images are generated.

In order to reduce CT dose, first, patients should be selected carefully. Inappropriate CT referrals should be eliminated. Second, range of scan should be limited to the area of interest. Unnecessary contrast phases should be eliminated. Using a large pitch, automated current modulation, adaptive dose shielding, and updated image reconstruction algorithms are other helpful techniques of CT dose reduction in craniofacial trauma.

Craniofacial Anatomy

Anatomically, the face is divided into upper, middle, and lower thirds (Fig. 17.1). The upper third is comprised of the frontal bone and extends to its zygomatic, maxillary, and nasal sutures. The middle third extends from the frontal bone to the upper teeth of the maxilla. The mandible represents the lower third. The "midface" is comprised of the maxilla, zygoma, nasal, lacrimal, vomer, inferior concha, and palatine bones (Table 17.1). The frontal, sphenoid, and ethmoid bones form portions of both the cranium and face. The facial bones are relatively weak owing to their multiple sinus cavities but are reinforced with a series of vertical and horizontal buttresses. They are able to withstand forces in the vertical direction but are much weaker in the horizontal and lateral directions. The goal of the surgeon is to restore alignment and integrity of these buttresses when they fracture. There are four vertical and four horizontal facial buttresses (variously termed struts of mastication, midfacial buttresses, or structural pillars).

Table 17.1 Craniofacial bones

Upper third	Middle third	Lower third
Frontal bone:	Maxilla	Mandible
– Zygomatic	Zygoma	
– Maxillary	Nasal	
– Nasal sutures	Lacrimal	
	Vomer	
	Inferior concha	
	Palatine	
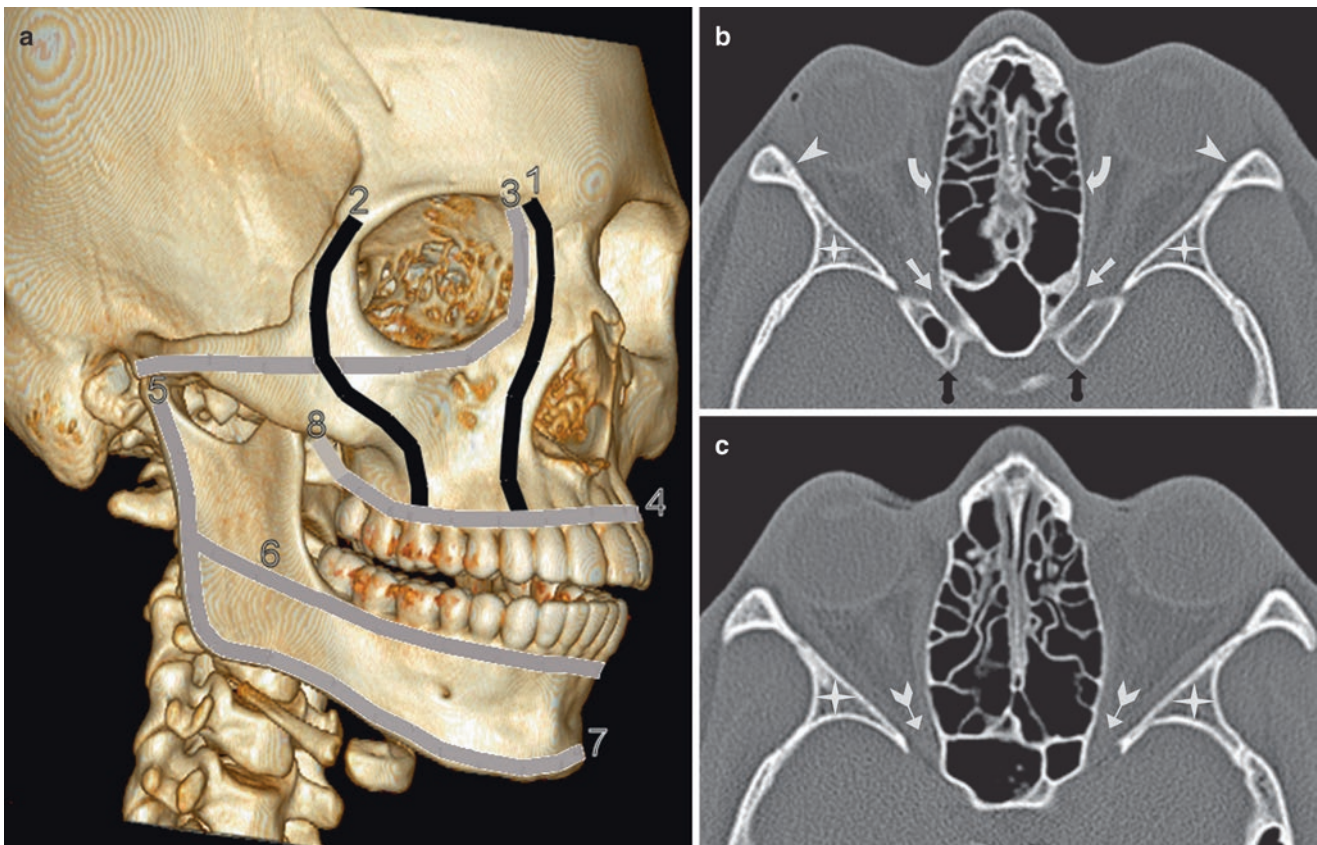
Fig. 17.1 Normal CT anatomy and facial buttresses. (**a**) 3D surface-rendered image demonstrating the four vertical and four transverse buttresses (*1* medial maxillary, *2* lateral maxillary, *3* upper transverse maxillary, *4* lower transverse maxillary, *5* posterior vertical, *6* upper transverse mandibular, *7* lower transverse mandibular, and *8* posterior maxillary). (**b**, **c**) Axial CT demonstrates the normal anatomy of the facial bones (*arrowhead* zygomatic arch, *curved arrow* laminae papyracea, *white straight arrow* optic canal, *black straight arrow* anterior clinoid process, *star* greater wing of sphenoid, and *white arrow* superior orbital fissure)

The floor of the anterior cranial fossa (ACF) is formed by the cribriform plate of the ethmoid, the frontal bone, and the lesser wing of the sphenoid. The frontal bone forms the majority of the floor of the ACF and also comprises the majority of the orbital roof. The lesser wing of the sphenoid forms the posterior margin of the ACF. The floor of the middle cranial fossa (MCF) is formed by the greater wing of the sphenoid and the squamosal portion of the temporal bone [7].
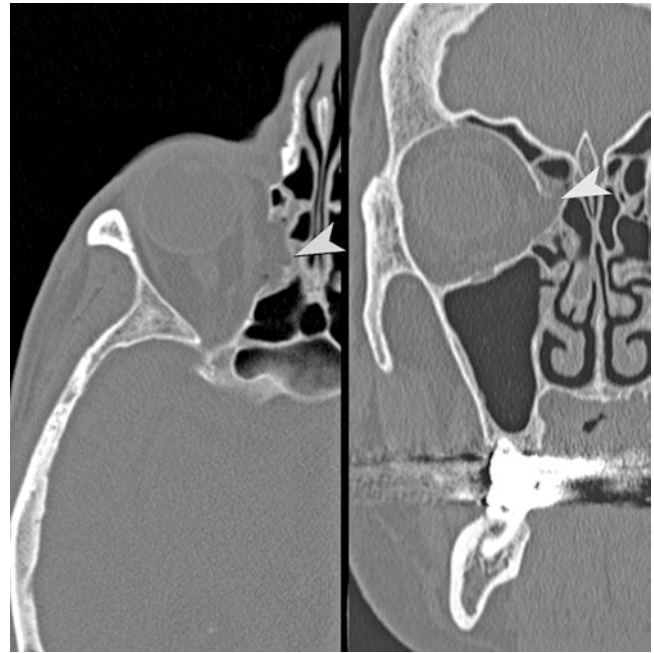
Orbital Fractures

The orbit is shaped like a cone with the apex posterior and the base anterior. The apex of the orbit is at the convergence of the superior and inferior orbital fissures. The anterior orbital rim is composed of the frontal, maxillary, and zygomatic bones.

Fractures of the orbit can affect the orbital rim, orbital walls, or orbital apex. Orbital apex fractures are an important fracture to detect due to proximity to the optic nerve and are more commonly seen with complex injury. The most common isolated orbital fractures are the so-called blow-out fractures that occur in the medial and inferior orbital walls.

Blow-Out Fractures

A blow-out fracture is a fracture of the orbital wall that displaces outwardly. In 1957 Smith and Regan proposed a mechanism of increased intraorbital pressure secondary to a direct frontal blow to the globe [8]. The forces are transmitted through the orbital walls with fracturing of the weakest sections while the orbital rim remains intact [9]. Enophthalmous may occur as a result of blow-out fractures and is best repaired after the edema has resolved. The lamina papyracea is the thinnest bone but is reinforced with buttressing from the ethmoid air cells. The inferior orbital wall is made weaker by the presence of the infraorbital groove and is the most common site of a fracture. The fracture fragment can displace inferiorly into the maxillary sinus, resulting in herniation of intraorbital fat, and/or extraocular muscles. The "trapdoor" blow-out fracture, which is more common in pediatric age group, occurs when the hinge fragment springs back into place often trapping the inferior rectus muscle. Entrapment of the inferior rectus muscle results in limitation of upward/outward gaze, while entrapment of the medial rectus muscle results in limitation in the lateral gaze.

The coronal and sagittal reformations are most useful for detecting orbital floor fracture. Axial and coronal images best detect fractures of the medial wall (Figs. 17.2 and 17.3). It is important to note the site of fracture, fracture displacement and/or fracture angulation, and the presence or absence of herniated orbital contents as they are predictors of

Fig. 17.2 Medial orbital wall blow-out fracture. Axial and coronal CT images demonstrate a fracture (*arrowhead*) of the right medial orbital wall (lamina papyracea). Note the herniation of orbital fat through the defect in the right medial orbital wall

Fig. 17.3 Orbital floor lateral hinge blow-out fracture. Coronal and sagittal images in bone and soft tissue algorithm demonstrating a right orbital floor blow-out fracture. The displaced fragment hinges laterally at the infraorbital fissure. Note herniation of the orbital contents (*arrowhead*), including the inferior rectus muscle

Fig. 17.4 Orbital roof blow-in fracture. Coronal and sagittal CT reformations demonstrate a "pure" orbital blow-in fracture (*arrowhead*) of the left orbital roof. The orbital rim is intact

persistent diplopia. Surprisingly, large fractures have a lower risk for entrapment, compared with small and medium sized orbital fractures.

Blow-in Fractures

The blow-in fracture is less common compared with blow-out fractures, and is defined as an inwardly displaced fracture of the orbital wall and/or rim resulting in a reduced orbital volume. These are generally the result of high-energy trauma and are most commonly seen in association with other fractures [10, 11]. A "pure" blow-in fracture is one limited to the orbital walls while the orbital rim remains intact (Figs. 17.4 and 17.5). "Impure" blow-in fractures, which are much more common, involve inward displacement of the orbital rim (Table 17.2). Superior rim fractures, owing to their location and higher-impact forces, are usually more severe and associated with head injuries and frontal sinus fractures. Inferomedial blow-in rim fractures are the most common and seen with NOE fractures. Blow-in fractures commonly lead to proptosis, and increase the risk of optic nerve injuries.

Fig. 17.5 Orbital rim blow-in fractures. Surface-rendered image demonstrating orbital rim blow-in fracture of the superomedial orbital rim associated with a frontal fracture (*arrowhead*)

Table 17.2 Blow-in fractures

Pure blow-in fracture	Limited to the orbital walls Orbital rim remains intact Less common
Impure blow-in fracture	Inward displacement of the orbital rim More common

Fractures of the orbital apex may result in superior orbital fissure syndrome [12]. Symptoms include diplopia, ophthalmoplegia, ptosis, proptosis, and anesthesia in the ophthalmic nerve distribution. If there is associated blindness due to optic nerve injury (optic canal), it is termed orbital apex syndrome.

Zygoma Fractures

The zygoma (malar bone) is a dense solid bone that articulates with the frontal, maxillary, sphenoid, and temporal bones and forms the malar prominence (cheek), an important component of the facial contour. Since the zygoma is a solid bone, a direct blow to the cheek usually results in fractures of its relatively weaker articulation points. As the majority of the lateral orbital wall is formed by the zygoma, fractures to this region usually involve the orbit.

Zygomaticomaxillary Complex Fractures

While it is also called malar, tripod, tetrapod, and zygomatic complex fracture, the generally accepted and most commonly used term is zygomaticomaxillary complex (ZMC) fracture. It has a tendency to fracture at the weaker articulations with the frontal, sphenoid, maxillary, and temporal bones, resulting in disruption of the lateral maxillary and upper transverse maxillary buttresses [13]. Fractures of the ZMC may result in increased or decreased orbital volume.

While damage to the infraorbital nerve will result in loss of sensation to the eyelid and lateral nose, injury to the zygomatic nerve will result in sensory impairment to the lateral midface. Displaced fractures may result in flattening of the malar prominence, facial asymmetry, and may require surgery. Treatment can be conservative in the mildly displaced fractures.

Because of its complex articulation, the ZMC fragment can rotate in any plane along the fracture lines. The goal of imaging is to evaluate the extent of the fractures, the position and displacement of the ZMC fragment, and the status of the zygomatic arch (Figs. 17.6 and 17.7). The fractures may be associated with ocular injuries.

Isolated Fractures

A focused direct blow may result in an isolated arch fracture. The direction of the force usually results in a depressed V-shaped fracture with the apex directed toward the infratemporal fossa. Segmented fractures may result as well (Fig. 17.8). Complications result from impingement of the temporal muscle and injury to the zygomatic nerve.

Nasal Fractures

The bridge of the nose is formed by the paired nasal bones, the frontal process of the maxilla, and the nasal processes of the frontal bone. The ethmoid is comprised of multiple delicate buttressing bones and air cells and is bounded laterally by the orbits and maxillary sinuses. The nasal septum is formed by the vertical plate of the ethmoid and vomer posteriorly and cartilaginous septum anteriorly. The lateral nasal wall is formed by three longitudinal elevations called conchae (turbinates). The superior and middle turbinates are part of the ethmoid, while the inferior turbinate is a separate bone.

Fractures of the nasal bones are the most common facial fractures seen in the emergency imaging of trauma cases. The nasal bones form a portion of the nasal bridge and, if fractured, may result in facial deformity. Injury can range from isolated nasal bone fractures to more complex patterns involving multiple bones (Figs. 17.9 and 17.10). Radiographs are still routinely ordered if there is suspicion of an isolated nasal fracture. On CT attention to the nasal septum is important to evaluate for the presence of a septal hematoma, which may lead to complications of ischemic necrosis or abscess formation. Associated anterior nasal spine fractures may be present. Close reduction may be possible immediately after trauma. Open reduction is done in comminuted fractures, severe injuries, and marked soft tissue damage. Presence of bone fragment in the maxillary sinus may cause sinusitis. Nasal septal hematoma may cause necrosis, saddle-nose deformity, and abscess formation.

Naso-Orbital-Ethmoid Fractures

A high-impact force to the central face may disrupt the medial maxillary and upper transverse maxillary buttresses, referred to as naso-orbital-ethmoid (NOE) fractures. They account for 15% of pediatric and 5% of adult facial fractures. A classification system developed by Markowitz and Manson is based on the degree of injury to the medial maxillary buttress at the insertion of the medial canthal ligament (Table 17.3) [14]. The posterior extension of the medial maxillary buttress is made up of thin delicate bones offering little support, which results in impaction and posterior telescoping of the midface. Depressed and displaced fractures may result in flattening of the nasal bridge and telecanthus. Frequency of NOE fractures has decreased due to routine airbag use.

Axial and coronal images provide the most information (Figs. 17.11 and 17.12). It is important to evaluate the medial maxillary buttress at the level of the lacrimal fossa, the site of medial canthal ligament attachment. Reconstruction of the attachment of the medial canthal ligament is essential to avoid telecanthus, enophthalmos, and dysfunction of the lacrimal system. It is also important to comment on the posterior extension of these buttresses—medial orbital walls and floor. Additional associated injuries may include nasofrontal duct injury, cribriform plate fracture, frontal sinus involvement, orbital apex involvement, and associated ocular injuries.

Frontal Fractures

The frontal bone progressively pneumatizes throughout childhood. The anterior table forms the forehead and the superior orbital rims. The posterior table forms the anterior wall of the anterior cranial fossa. This strong bone forms the transverse frontal buttress and provides the anchor for the vertical maxillary buttresses. Due to its strength, a large force is required to fracture the frontal bone [15]. The frontal
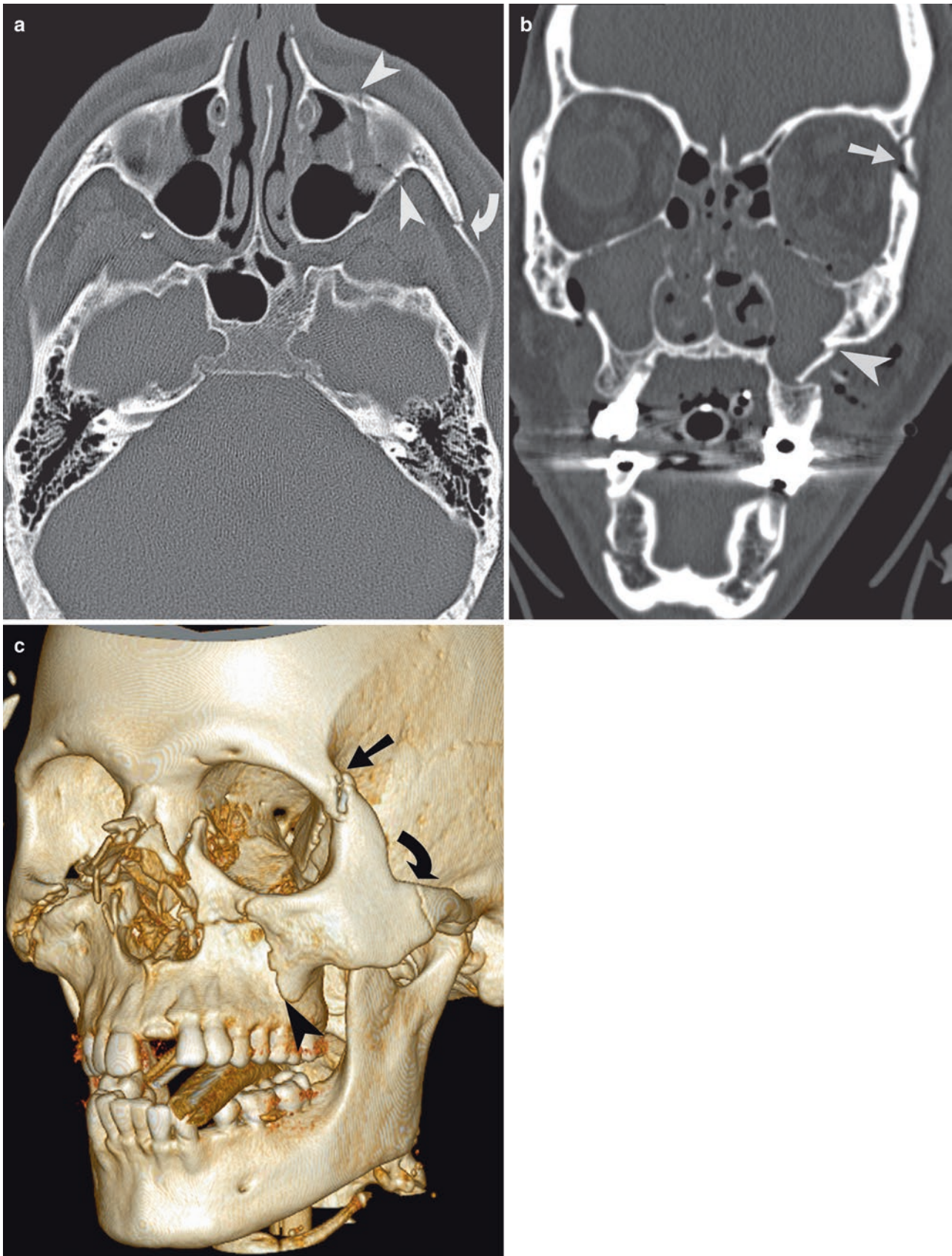
Fig. 17.6 ZMC fracture. (**a**, **b**) Axial and coronal CT demonstrates fractures of the anterior/posterolateral antral walls (*arrowheads*), orbital floor, lateral orbital rim, and 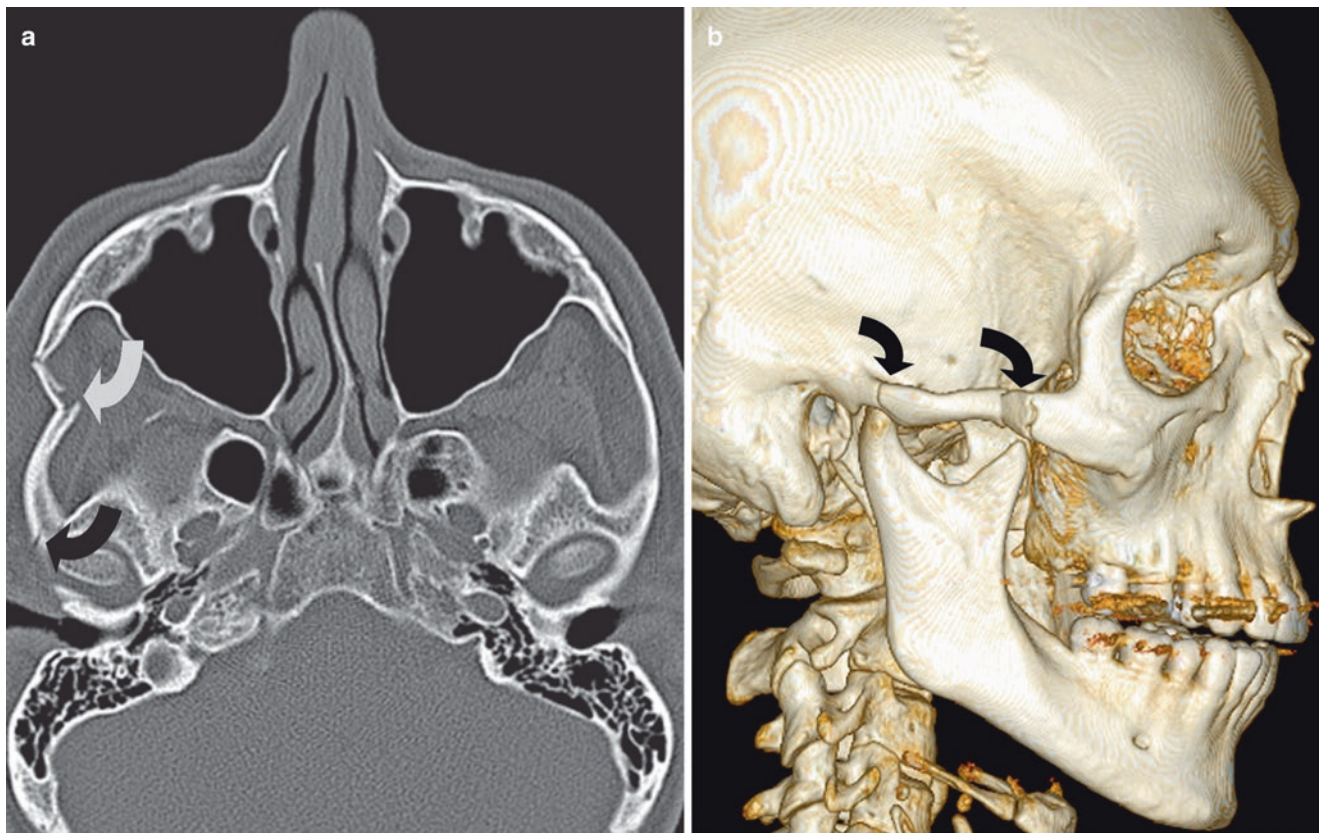zygomatic arch (*curved arrow*). (**c**) Surface-rendered image demonstrates fractures of the left zygomatico-temporal suture (*curved arrow*), zygomaticofrontal suture (*straight arrow*), and zygomaticomaxillary suture (*arrowhead*)
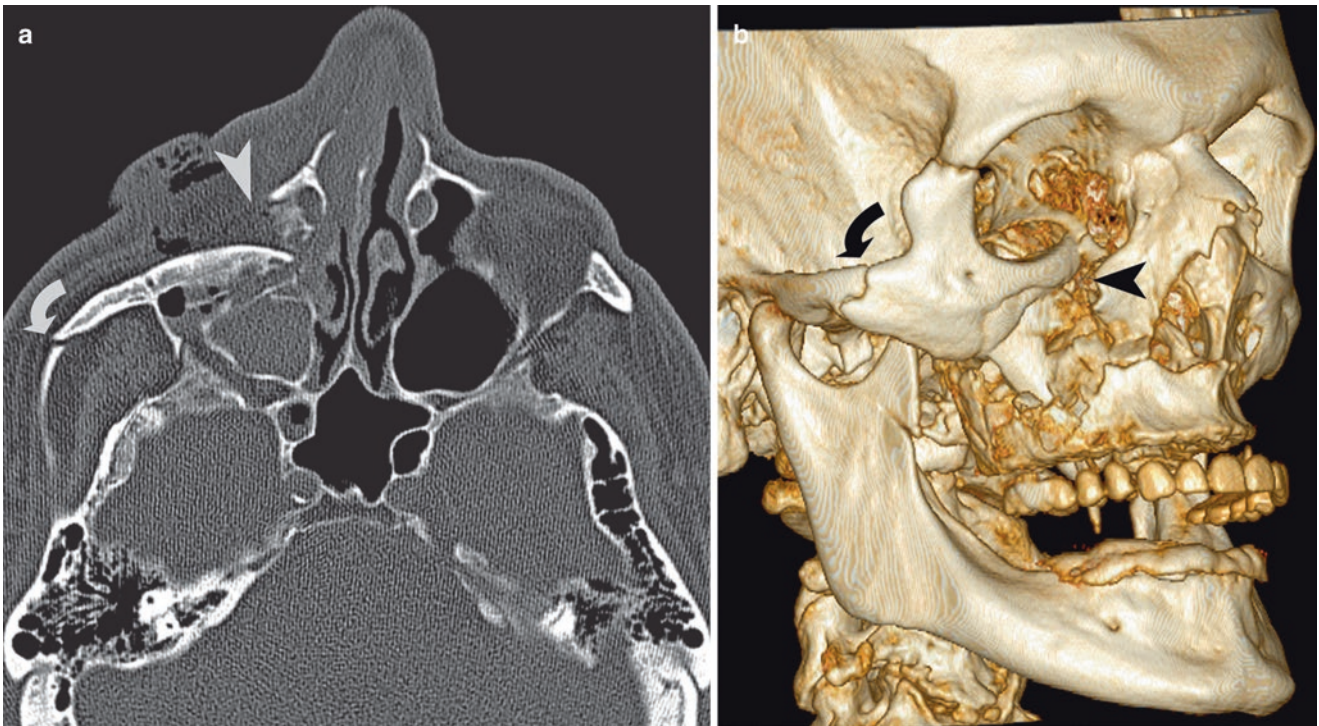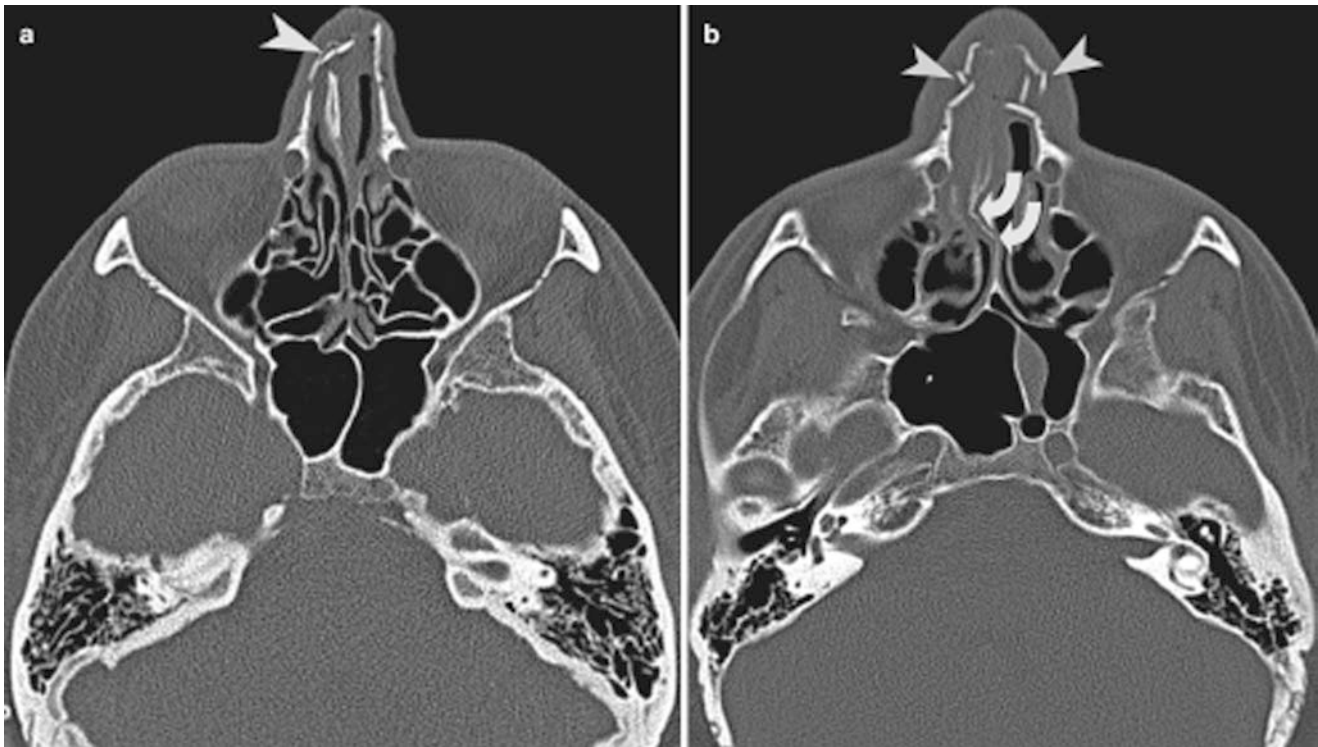
Fig. 17.7 Displaced and angulated ZMC fracture. (**a**, **b**) Axial image and surface-rendered image showing the zygoma complex posterolaterally displaced and internally rotated with displaced zygomaticomaxillary fracture (*arrowheads*) and zygomaticotemporal fracture (*curved arrows*). There is also fracture of the coronoid process of the mandible


Fig. 17.8 Zygomatic arch fracture. (**a**, **b**) Axial CT and surface-rendered image demonstrates a depressed, segmental fracture of the zygomatic bone (*curved arrows*)

Fig. 17.9 Nasal bone fracture. (**a**) Axial CT demonstrates comminuted, displaced, and angulated right nasal bone fractures (*arrowhead*). (**b**) Axial CT demonstrates fractures that involve the nasal bones (*arrowheads*), frontal process of the maxilla, and nasal septum (*curved arrows*). Note posterior displacement with telescoping of the nasal septum
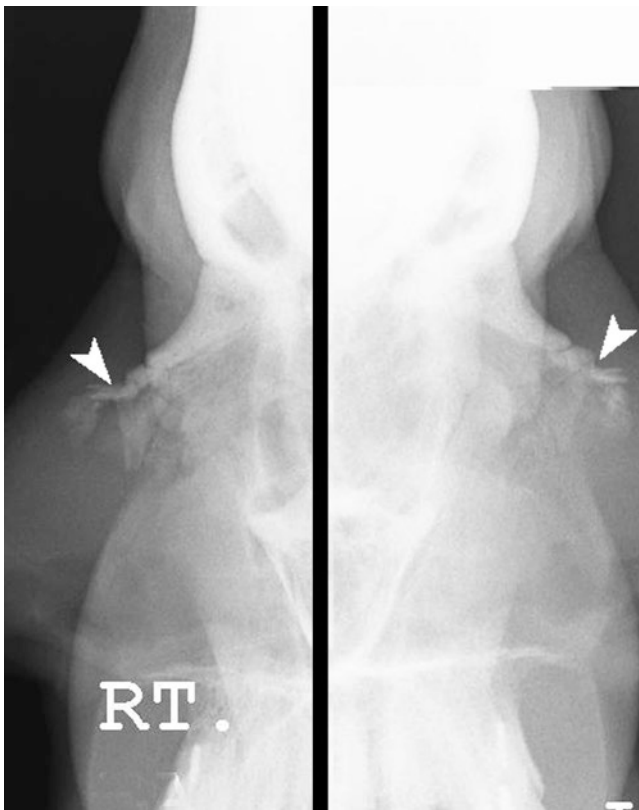
Fig. 17.10 Nasal bone fractures. Lateral view radiographs demonstrate comminuted fractures of bilateral nasal bones

**Table 17.3** Manson classification of NOE fractures

Type 1	Most common Single fragment
Type 2	Comminuted Intact insertion of medial canthal tendon
Type 3	Uncommon Comminuted Lateral displacement or avulsion of medial canthal ligament

sinus drains to the nose via the nasofrontal ducts. Injury to the nasofrontal duct can lead to later complications including frontal sinus mucocele, frontal sinusitis, osteomyelitis with anaerobes or intracranial extension leading to brain abscess. Complications may develop years after the trauma. Surgeons may obliterate the frontal sinus (cranialization) to prevent these complications [16, 17].

Depressed outer table fractures will result in forehead deformities although this may be masked by the edema. Fractures of the posterior table are rarely isolated and may result in dural tear and CSF rhinorrhea. Fractures of the cribriform plate may result in anosmia. Fractures of the lateral frontal sinus floor usually involve the orbital roof.

CT is important to evaluate the extent of the fracture and whether it involves the anterior table, posterior table, or both (Figs. 17.13 and 17.14). When evaluating posterior table fractures, one should look for displacement, depression,
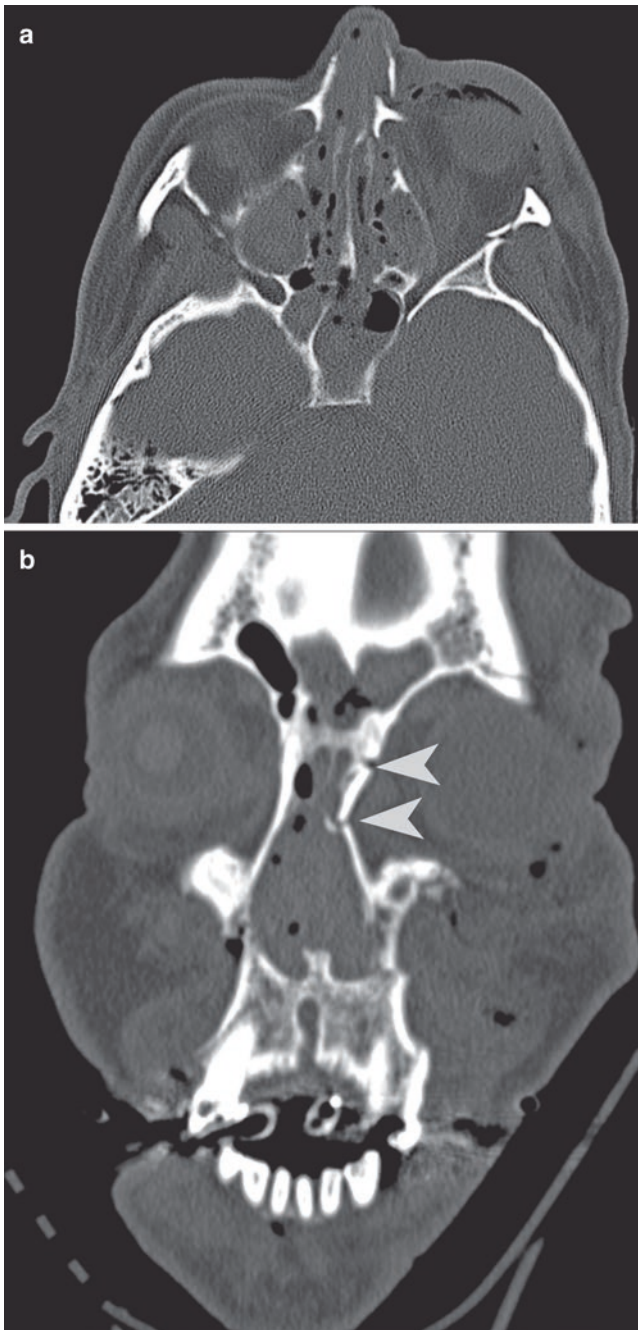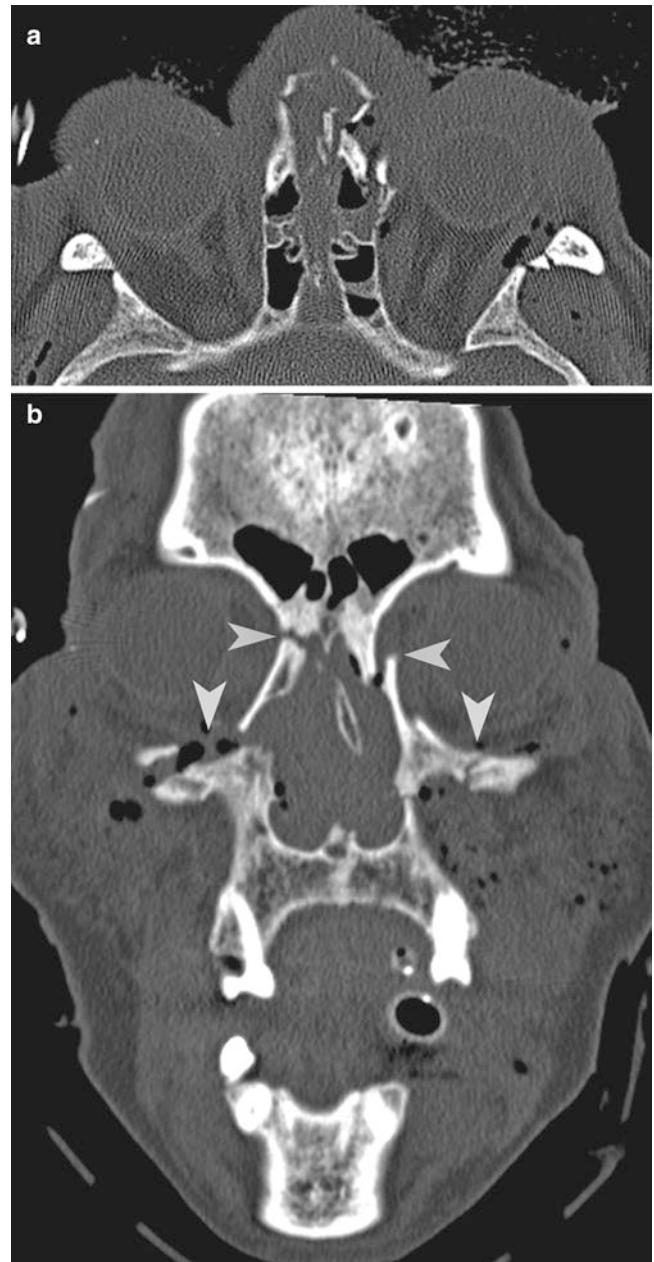
Fig. 17.11 Naso-orbital-ethmoid (NOE) fracture. (**a**) Axial CT image at the level of the lacrimal fossa demonstrates a comminuted fracture and disruption of the left medial maxillary buttress. (**b**) Coronal images at the level of the lacrimal fossa demonstrating disruption of the left medial maxillary buttress (*arrowheads*)

Fig. 17.12 NOE fracture. (**a**, **b**) Axial and coronal CT image in a patient with facial smash injury demonstrates NOE, Le Fort II (*arrowheads*), and bilateral ZMC fractures. The fractures have resulted in disruption of the medial maxillary, lateral maxillary, and upper transverse buttresses. There is posterior displacement of the central face and lateral displacement of the medial maxillary buttresses

pneumocephalus (suggesting dural disruption), and intracranial injury.

Management has become increasingly conservative. A patent outflow tract indicates salvageable frontal sinus. If the outflow tract cannot be restored, the sinus is eradicated. Posterior table fractures may need to be cranialized. Follow-up with CT scans to exclude possible complications may be useful.

Maxillary Fractures

The maxilla, palatine, and nasal bones form the majority of the midface. The anterior maxillary wall forms the flat portion of the face between the nose and cheek. The maxilla contains the maxillary antrum which is bordered by thin walls, resulting in predictable fracture patterns.

Fig. 17.13 Anterior and posterior table frontal fractures. Axial CT and surface-rendered images demonstrate comminuted fractures involving both the anterior and posterior tables (*arrowheads*). Pneumocephalus suggests dural disruption (*straight arrow*)
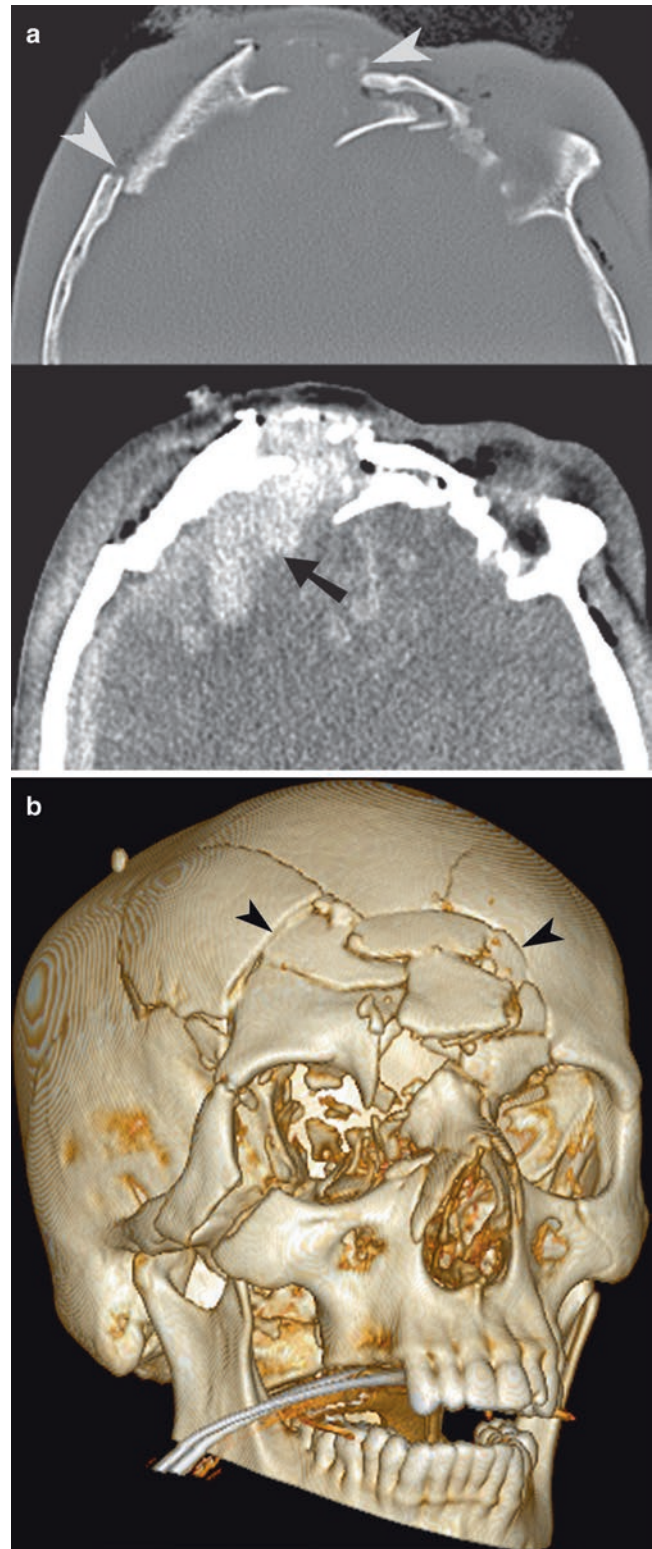
Le Fort Fractures

In 1901 Rene Le Fort published results of experiments performed on cadavers in which he demonstrated predictable fracture patterns of the midface [1]. Le Fort fractures are often seen in combination with other fractures [18].

Le Fort type I fractures result from trauma at a level immediately superior to the alveolar process of the maxilla. The horizontal fracture line extends through the anterior maxillary wall, medial antral wall, lateral antral wall, and pterygoid plates. There is depression of the lower transverse maxillary buttress, the hard palate. Type I fractures disrupt both medial and lateral maxillary buttresses (Fig. 17.15).

Le Fort type II fractures result from trauma at the level of the nasal bones with disruption of the (inferior) lateral and (superior) medial maxillary buttresses. These are also referred to as pyramidal fractures, with the entire maxilla moving with respect to the skull base. Type II fractures extend across the nasal bridge, the inferomedial orbital rim, and zygomaticomaxillary suture and posteriorly through the maxillary sinus to the level of the pterygoid plates (Fig. 17.16).

Le Fort type III fractures result from a force delivered at the orbital level. The (superior) medial, (superior) lateral,

Fig. 17.14 Comminuted frontal fracture with intracranial injury. (**a**, **b**) Severely comminuted open frontal bone fractures (*arrowheads*) with associated intracranial subdural hemorrhage and frontal lobe contusion (*straight arrow*)
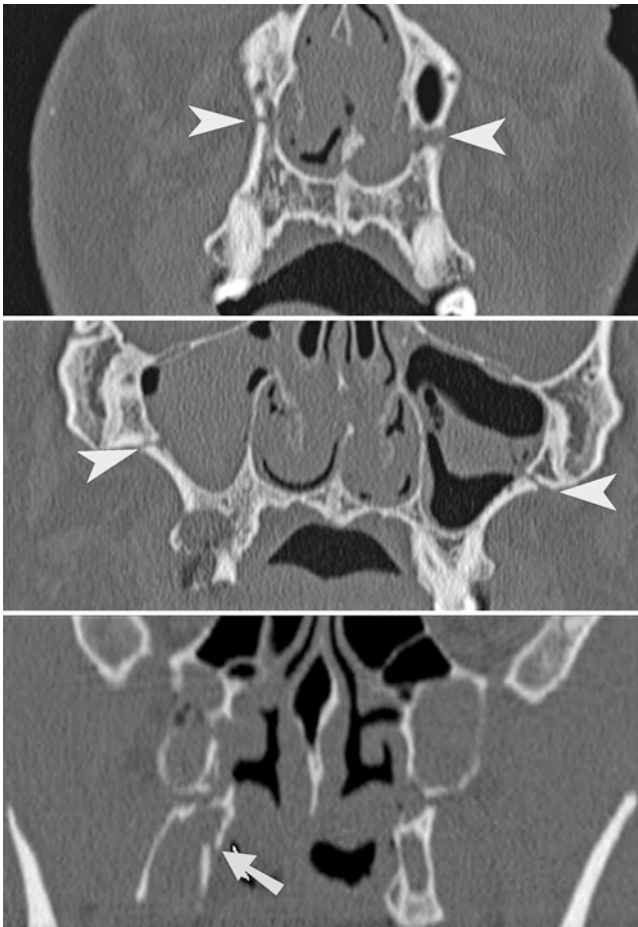
Fig. 17.15 Le Fort I fracture. Sequential coronal images from anterior to posterior showing a horizontal fracture through the medial maxillary buttresses (*arrowheads*), medial and lateral antral walls (*arrowheads*), and extending to the pterygoid plates (*straight arrow*)

and upper transverse maxillary buttresses are disrupted, resulting in craniofacial dissociation. The fracture line extends across the nasal bridge, zygomaticofrontal suture, zygomaticotemporal suture, and orbital walls, terminating posteriorly at the level of the pterygopalatine fossa, pterygoid process, or pterygoid plates. It is distinguished from the ZMC fracture by involvement of the medial orbital wall and posterior extension (Fig. 17.17).

Type I fractures may result in a free-floating palate. Type II injuries may demonstrate step deformities at the nasal bridge and infraorbital rim. Type III injuries may demonstrate craniofacial instability. With posterior displacement, Type II and III injuries may demonstrate the characteristic "dish-face" deformity, a concave appearance of the face.

Type I injuries can be associated with dentoalveolar and mandible fractures. Type II and III injuries often demonstrate associated ZMC and NOE fractures. Type III injuries can be associated with skull fractures and intracranial injuries. Table 17.4 summarizes Le Fort fractures.
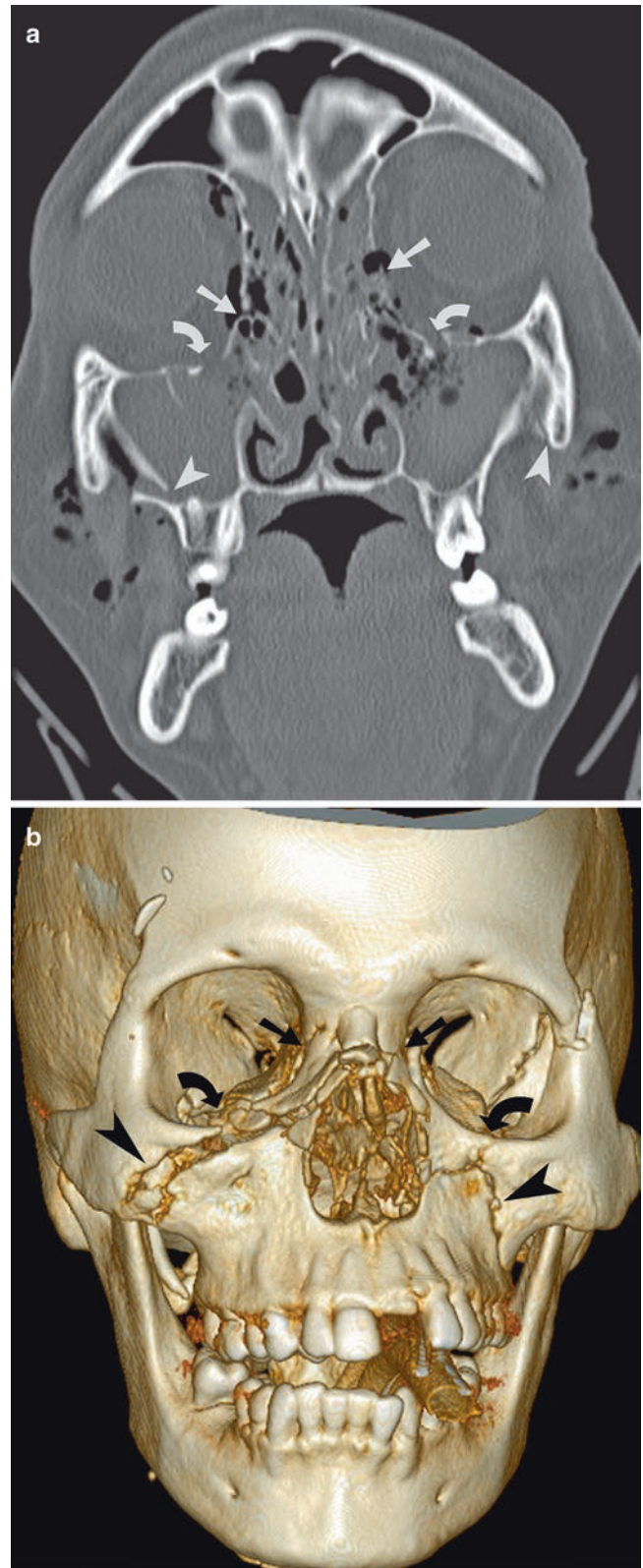
Fig. 17.16 LeFort II fracture. (**a**, **b**) Coronal CT reformation and surface-rendered image demonstrate multiple comminuted pyramid-shaped fracture of the mid face. There are fractures of medial orbital walls (*straight arrow*), orbital floor (*curved arrows*), and lateral antral wall (*arrowhead*)
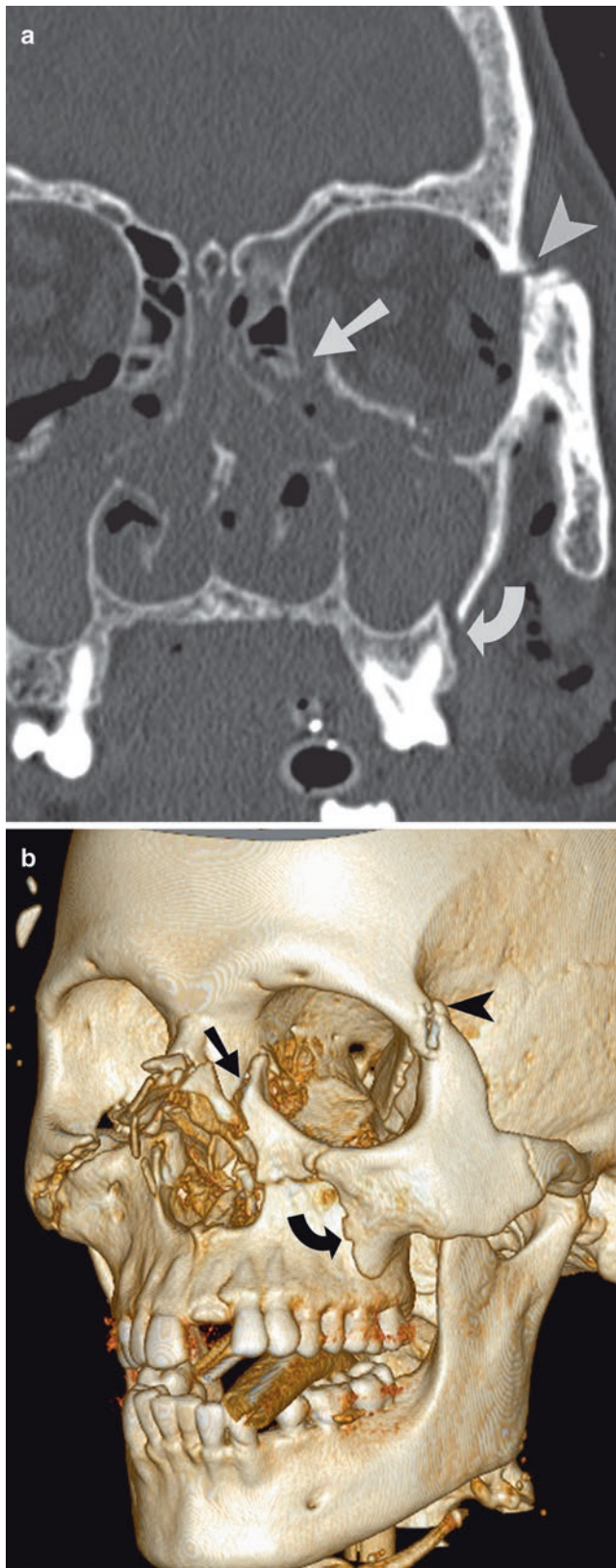
Fig. 17.17 Left Hemi-LeFort II and III fracture. (**a**, **b**) Coronal CT reformation and surface-rendered image demonstrates fractures through the left medial orbital wall (*straight arrow*), orbital floor, lateral antral wall (*curved arrow*) and zygomaticofrontal suture (*arrowhead*). The posterior extension and involvement of the posteromedial orbital wall distinguishes these fractures from the ZMC fracture

Table 17.4 Le Fort fractures

	Type I	Type II	Type III
Trauma level	Superior to the alveolar process of the maxilla	Nasal bones with disruption of the lateral and medial maxillary buttresses	Orbital level
Disruption	Medial and lateral maxillary buttresses	Inferior lateral and superior medial maxillary buttresses	Superior medial, lateral, and upper transverse maxillary buttresses
Results	Free-floating palate	Step deformities at the nasal bridge and infraorbital rim Possibly "dish-face" deformity	Craniofacial instability Possibly "dish-face" deformity
Associated injuries	Dentoalveolar and mandible fractures	ZMC and NOE fractures	ZMC and NOE fractures Skull fractures and intracranial injuries

Dentoalveolar and Maxillary Sagittal Fractures

The hard palate is formed by the horizontal process of the maxilla and palatine bone. Fractures may affect the alveolus and/or palate in isolation or in combination with other more complex fractures [19, 20]. The World Health Organization (WHO) has developed an injury classification system of dentoalveolar fractures:

- Fracture of the tooth: enamel infraction, enamel fracture, enamel-dentin fracture, complicated crown fracture, uncomplicated crown-root fracture, complicated crown-root fracture, root fracture
- Injury to the periodontal tissue: concussion, subluxation (loosening), extrusive luxation(peripheral dislocation, peripheral avulsion), lateral luxation, intrusive luxation (central dislocation), avulsion (exarticulation)
- Injury to the supporting bone: comminution of the mandibular, fracture of the mandibular or maxillary alveolar socket wall, fracture of the mandibular or maxillary alveolar process, jaw fracture
- Injuries to the gingival or oral mucosa: laceration of gingival or oral mucosa, contusion of gingiva or oral mucosa, abrasion of gingival or oral mucosa [21].

A classification system of maxillary sagittal fractures, developed by Hendrickson, is based on the fracture pattern through the palate:

I. Anterior and posterolateral alveolar
II. Sagittal

III. Parasagittal
IV. Para-alveolar
 V. Complex
VI. Transverse [22].

Palatal fractures are commonly associated with Le Fort I (100%), Le Fort II and III (55%), dental (55%), and mandible (48%) fractures.

Clinically, the presence of mobility of multiple teeth suggests a fracture of the alveolar process. Facial, chest, and abdominal radiographs may be helpful to evaluate for displaced, swallowed, or aspirated teeth and bone fragments. Panoramic radiographs can evaluate the teeth and the integrity of the periodontal ligament. When evaluating CT scans with dentoalveolar injury, it is important to note fractures of teeth, dental extrusion or intrusion, displacement, tooth socket fractures, tooth fragments lodged in soft tissues, and associated mandibular or other facial fractures.

Mandible Fractures

The mandible is formed by a horizontal U-shaped body and two vertical rami. The alveolar process arises from the body and contains the mandibular teeth. The superior portion of each ramus has two processes: a posterior condylar process and an anterior coronoid process, separated by the mandibular notch. The body and rami join at the angle of the mandible. The prominent position of the mandible in the lower third of the face makes it vulnerable to fracture. They commonly occur bilateral. The mandible fractures can be divided into the following regions: symphyseal, parasymphyseal, alveolar, body, angle, ramus, condylar process, and coronoid processes. Condylar process fractures are common, particularly the neck. In the setting of bilateral parasymphyseal fractures, the genioglossus, geniohyoid, and digastric muscles retract the symphysis posteriorly and inferiorly. The condylar head is often displaced medially in patients with condylar neck fractures due to the unopposed action of the lateral pterygoid muscle. CT angiogram of neck is indicated in fracture dislocation of condyle to assess for vascular injuries such as dissection.

As with most current imaging of craniofacial trauma, MDCT acquisition with axial, coronal, sagittal, and 3D volume-rendered reformats allows complete evaluation of mandibular fractures as well as associated injuries (Figs. 17.18 and 17.19). Treatment consists of intermaxillary (maxillomandibular) fixation, repair of the anterior segment (teeth-bearing, symphysis, and body), and reducing the posterior mandible (angle, ramus, coronoid, and condyle).

Questions

1. Which of the following statements is correct?
   (a) Impure blow-in orbital fractures are limited to the orbital walls
   (b) Pure blow-in orbital fractures are more common than impure fractures
   (c) Superior rim fractures are usually more severe
   (d) Nasal bone fractures are the second most imaged fractures in emergency setting

   Answer: C

2. Which of the following statements is correct regarding Manson classification of naso-orbital-ethmoid fractures?
   (a) Type 2 is the most common type
   (b) Type 2 consists of a single fragment
   (c) In Type 1 insertion of medial canthal tendon is intact
   (d) Type 3 involves lateral displacement or avulsion of medial canthal ligament

   Answer: D

3. Which of the following injury pattern is classically associated fracture with palatal fractures?
   (a) Le Fort I
   (b) Le Fort II
   (c) Le Fort III
   (d) Le Fort IV

   Answer: A

4. What is the abnormality detected on the volume-rendered CT depicted below (Fig. 17.20)?
   (a) Le Fort I
   (b) Zygomaticomaxillary complex fracture
   (c) Naso-orbital-ethmoid fracture
   (d) Mandibular fracture

   Answer: B

5. In a patient with history of motor vehicle collision (Fig. 17.21a, b) how would you characterize his mid facial fractures?
   (a) Le Fort I
   (b) Le Fort II
   (c) Le Fort III
   (d) Both Le Fort II and III

   Answer: D
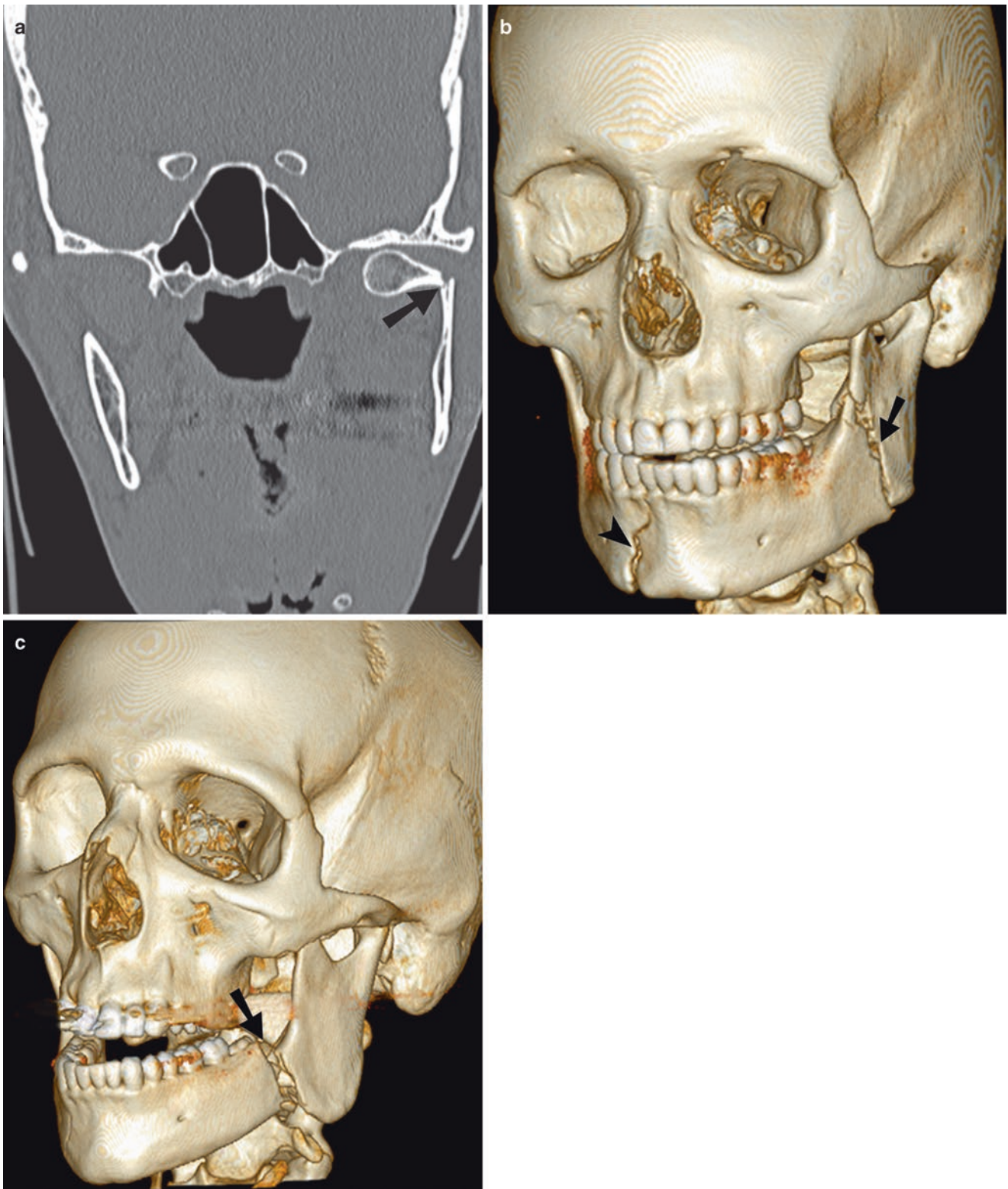
Fig. 17.18 Mandible fractures. (**a**) Coronal CT reformation shows angulated subcondylar fracture (*straight arrow*) with medial dislocation of the left mandible condyle head. (**b**) Surface-rendered CT image demonstrates right parasymphyseal (*arrowhead*) and left mandibular angle (*straight arrow*) fractures. (**c**) Surface-rendered CT image demonstrates displaced left mandibular angle fracture (*straight arrow*)
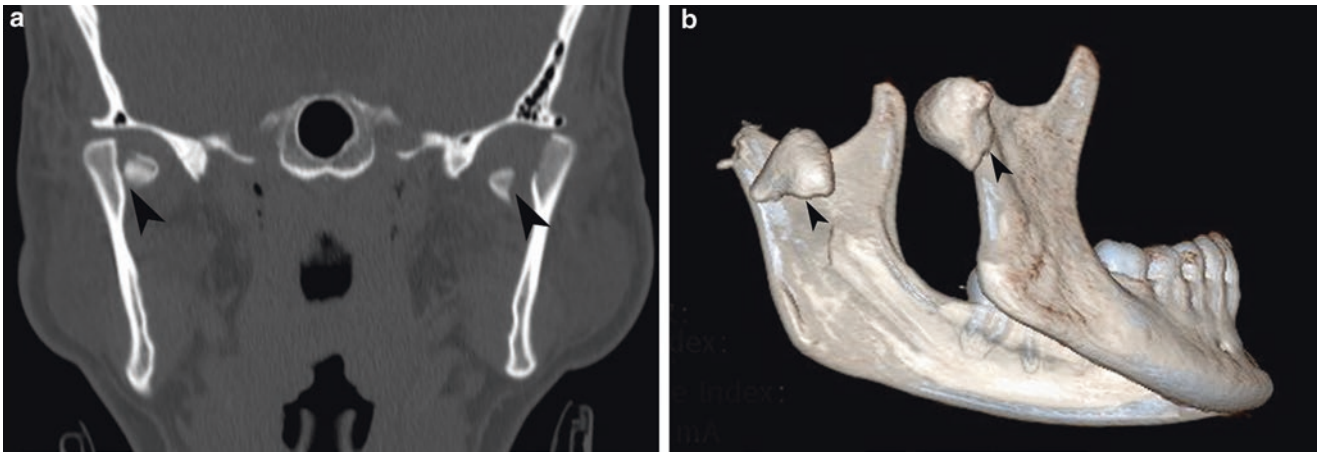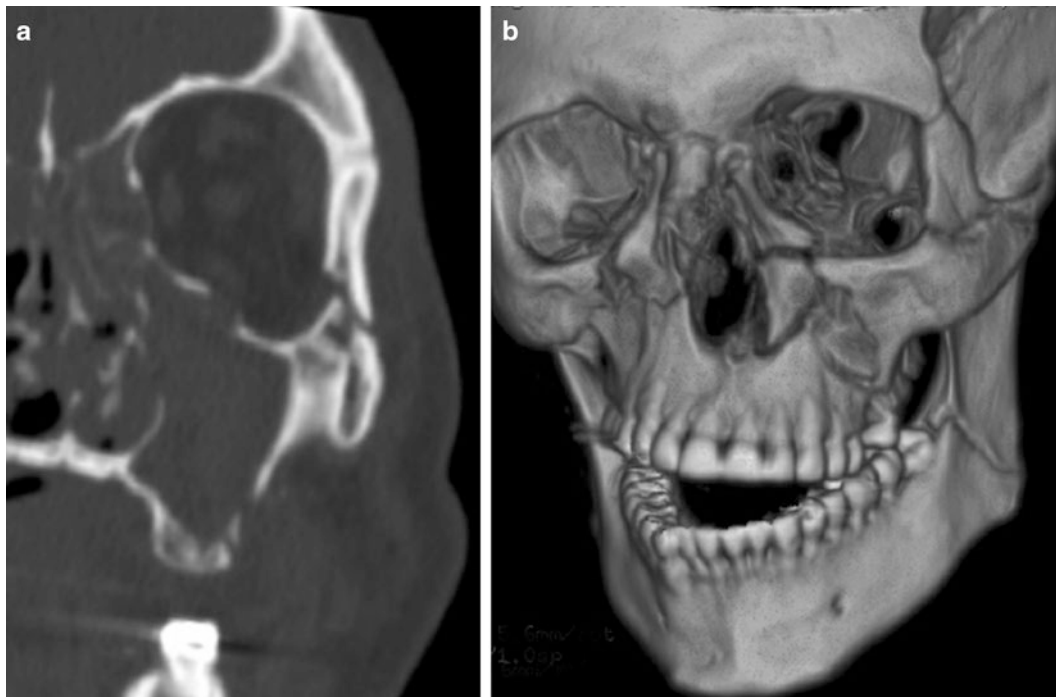
Fig. 17.19 Bilateral mandible subcondylar fractures. CT demonstrates bilateral subcondylar fractures on coronal (**a**) and surface-rendered images (**b**)

Fig. 17.20

Fig. 17.21

References

1. LeFort R. Etude experimentale sur les fractures de la machoire superieure. Rev Chir. 1901;23:208–27.
2. Sicher H, Debrul EL. Oral anatomy. 5th ed. St. Louis: Mosby; 1970. p. 78.
3. Gentry LR, Manor WF, Turski PA, Strother CM. High resolution of the CT analysis of the facial struts in trauma: 1 and 2: normal anatomy and osseous and soft-tissue complications. AJR Am J Roentgenol. 1983;140:523–32.
4. Manson P, Hoopes JE, Su CT. Structural pillars of the facial skeleton: an approach to the management of le fort fractures. Plast Reconstr Surg. 1980;66(1):54–61.
5. Fonseca R, Barber HD, Powers M, Frost DE. Oral and maxillofacial trauma. St. Louis: Elsevier/Saunders; 2005.
6. Dolan K, Jacoby CG, Smoker WRK. The radiology of facial fractures. Radiographics. 1984;4:575–663.
7. Moore K, Dalley AF, AMR A. Clinically oriented anatomy. 6th ed. Baltimore: Lippincott Williams & Wilkins; 2010.
8. Smith B, Regan WF. Blow-out fracture of the orbit, mechanism and correction of internal orbital fracture. Am J Ophthalmol. 1957;44:733–9.
9. Rhee J, Kilde J, Yoganadan N, Pintar F. Orbital blowout fractures: experimental evidence for the pure hydraulic theory. Arch Facial Plast Surg. 2002;4:98–101.
10. Chirico P, Mirvis SE, Kelman SE, Karesh JW. Orbital "blow-in" fractures: clinical and CT features. J Comput Assist Tomogr. 1989;13(6):1017–22.
11. Antonyshyn O, Gruss JS, Kassel EE. Blow-in fractures of the orbit. Plast Reconstr Surg. 1989;84(1):10–20.
12. Rohrich RJ, Hackney FL, Parikh RS. Superior orbital fissure syndrome: current management concepts. J Craniomaxillofac Trauma. 1995;1(2):44–8.
13. Hopper R, Salemy S, Sze RW. Diagnosis of midface fractures with CT: what the surgeon needs to know. Radiographics. 2006;26:783–93.
14. Markowitz B, Manson PN, Sargent L, Vander Kolk CA, Yaremchuk M, Glassman D, et al. Management of the medial canthal tendon in nasoethmoid orbital fractures: the importance of the central fragments in classification and treatment. Plast Reconstr Surg. 1991;87(5):843–53.
15. Ioannides C, Freihofer HP. Fractures of the frontal sinus: classification and its implications for surgical treatment. Am J Otolaryngol. 1999;20(5):273–80.
16. Stanley R, Becker TS. Injuries of the nasofrontal orifices in frontal sinus fractures. Laryngoscope. 1987;97(6):728–31.
17. Gonty A, Marciani RD, Adornato DC. Management of frontal sinus fractures: a review of 33 cases. J Oral Maxillofac Surg. 1999;57:372–9.
18. Fraioli R, Branstetter BF 4th, Deleyiannis FW. Facial fractures: beyond le fort. Otolaryngol Clin N Am. 2008;41:51–76.
19. Andreasen JO, Bakland LK, Flores MT, Andreasen FM, Andersson L. Traumatic dental injuries: a manual. 3rd ed. Malden: Wiley-Blackwell; 2011. p. 260–2.
20. Antoniades K, Dimitriou C, Triaridis C, Karabouta I, Layaridis N, Karakasis D. Sagittal fracture of the maxilla. J Craniomaxillofac Surg. 1990;18(6):260–2.
21. World Health Organization. Application of the international classification of diseases to dentistry and stomatology. IDC-DA. 3rd ed. Geneva: World Health Organization; 1995.
22. Hendrickson M, Clark N, Manson PN, Yaremchuk M, Robertson B, Slezak S, et al. Palatal fractures: classification, patterns and treatment with rigid internal fixation. Plast Reconstr Surg. 1998;101:319–32.